THE JOURNAL OF PHYSICAL CHEMISTRY B

Article

pubs.acs.org/JPCB

Single Molecular Recognition Force Spectroscopy Study of a Luteinizing Hormone-Releasing Hormone Analogue as a Carcinoma Target Drug

Jing Zhang,[†,‡,#] Guangmou Wu,[§,#] Chunli Song,[∥] Yongjun Li,[†,‡] Haiyan Qiao,[†,‡] Ping Zhu,[§] Peter Hinterdorfer,[⊥] Bailin Zhang,*[,†] and Jilin Tang*[,†]

[†]State Key Laboratory of Electroanalytical Chemistry, Changchun Institute of Applied Chemistry, Chinese Academy of Sciences, Changchun, 130022, P. R. China

[‡]Graduate School of Chinese Academy of Sciences, Beijing, 100049, P. R. China

[§]Institute of Military Veterinary, Academy of Military Medical Sciences, Changchun, 130122, P. R. China

[∥]Department of Cardiology, The Second Hospital of Jilin University, Changchun, 130041, P. R. China

[⊥]Institute for Biophysics, Christian Doppler Laboratory of Nanoscopic Methods in Biophysics, Johannes Kepler University Linz, Linz, A-4040, Austria

Supporting Information

ABSTRACT: The luteinizing hormone-releasing hormone-*Pseudomonas aeruginosa* exotoxin 40 (LHRH-PE40), is a candidate target drug associated with elevated LHRH receptor (LHRH-R) expression in malignant tumor tissue. The capability of LHRH-PE40 to recognize LHRH-Rs on a living cell membrane was studied with single molecular recognition force spectroscopy (SMFS) based on atomic force microscopy (AFM). The recognition force of LHRH-PE40/LHRH-R was compared with that of LHRH/LHRH-R by dynamic force spectroscopy. Meanwhile, cell growth inhibition assay and fluorescence imaging were presented as complementary characterization. The results show that LHRH moiety keeps its capability to recognize LHRH-R specifically, which implies that recombinant protein LHRH-PE40 can be a promising target drug.

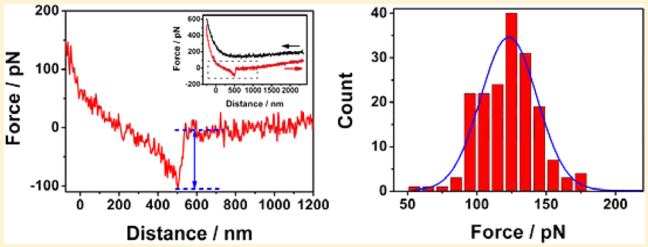

1. INTRODUCTION

The effective treatment of cancer with target drugs remains one of the major challenges in oncology. Cancer targeting is usually achieved by adding a ligand moiety to a drug delivery system, which will specifically direct to certain types of binding sites on cancer cells, such as receptors.[1] In the past decades, research efforts have begun to develop new selective anticancer drugs with less cytotoxic side effects.[2−7] Luteinizing hormone-releasing hormone (LHRH), also known as gonadotripin-releasing hormone 1 (GnRH 1), is a peptide hormone responsible for the release of follicle-stimulating hormone and luteinizing hormone from the anterior pituitary. It is a single, nonglycosylated, polypeptide chain (Pyr-His-Trp-Ser-Tyr-Gly-Leu-Arg-Pro-Gly-NH_2). Dharap and Minko[8] found that the receptors for LHRH (LHRH-Rs) are overexpressed in breast, ovarian, and prostate cancer cells. However, these receptors are not expressed at a detectable level in most visceral organs, including liver, kidney, spleen, heart, lung, brain, thymus, and skeletal. The elevated LHRH-R levels in malignant cancer tissues make them highly sensitive to the mitogenic and antiapoptotic activity of LHRH.[1] On the basis of the find, LHRH could be used as a targeting moiety in drug delivery system to enhance drug uptake by malignant cancer cells and reduce the relative availability of toxic drug to normal cells. As a promising anticancer target drug, LHRH-*Pseudomonas aeruginosa* exotoxin 40 (LHRH-PE40) was constructed by the fusion of both LHRH and PE40 genes with genetic engineering in vitro. The active principle of LHRH-PE40 is that the guide fraction LHRH binds to LHRH-R on targeted cell membrane surface, and then the toxic fraction PE40 enters cells through transmembrane transport to kill cancer cells.[9] As the basis for the toxicity of LHRH-PE40, the combination of LHRH moiety with LHRH-R is restricted by LHRH configuration. Whether the recombinant protein, LHRH-PE40, reserves the ability to bind to LHRH-R, is one of the key issues in drug targeting. The present study focuses on evaluating the specific binding of LHRH-PE40 to LHRH-Rs on target cell membranes.

To quantitatively determine the interaction strength of ligands and their receptors, force spectroscopy assays are considered particularly useful.[10] Single molecular recognition force spectroscopy (SMFS) is a newly developed atomic force microscopy (AFM) technique that measures binding force

Received: July 11, 2012
Revised: October 23, 2012
Published: October 24, 2012

governing biomolecular interaction at single-molecule level. As it is advantageous in performing in buffer solution and being minimally disruptive to living cells, it has become a powerful tool to probe the affinity and recognition property of a variety of biomolecular interactions not only in vitro but also in living cells.[11−20] Knowledge of these forces contributes to refine out understanding of the molecular basis of molecular recognition events such as those mediating cell adhesion and the immunological process.

Herein, the prospect of LHRH-PE40 as a carcinoma target drug was explored by AFM-based SMFS. The binding forces between the tethered LHRH-PE40 and its target on living cell membrane have been characterized at the single-molecule level. The recognition force of LHRH-PE40/LHRH-R was compared with that of LHRH/LHRH-R by dynamic force spectroscopy. The results show that the recombinant protein LHRH-PE40 keeps LHRH moiety's ability to bind to LHRH-Rs on a living cell surface. Also, cell growth inhibition assay and fluorescence imaging were presented as references. These results constitute a quantitative report on the use of AFM-based SMFS for the biodiscovery of new target drugs.

2. EXPERIMENTAL SECTION

2.1. Materials. The recombinant protein LHRH-PE40 was constructed by the fusion of both LHRH and truncated *Pseudomonas aeruginosa* exotoxin A (PEA) with genetic engineering technology and expressed in *Escherichia coli* BL21 (DE3). Then LHRH-PE40 was purified by anion exchange chromatography and hydrophobic interaction chromatography and identified by mass chromatographic analysis. Briefly, single colonies of *E. coli* BL21 transformed with LHRH-PE40 plasmids were grown in LB medium supplemented with ampicillin (50 μg mL^{-1}) at 37 °C until culture reached an OD_{600} of approximately 0.6, and were then induced by addition of 1 mM isopropylthiogalactoside (IPTG). Cells after 4 h of additional cultivation were collected by centrifugation for 1 min at 15 000*g*. Then 6 g of the cells were suspended in 15 mL of 25 mM Tris/HCl buffer (pH 8) containing 150 mM NaCl and 1 mM PMSF (Roche) and lysed by sonicating in ice bath for 20 s four times, taking care to avoid frothing. The lysate was centrifuged at 4 °C for 20−30 min at 15 000*g* to remove cellular debris, and the supernatant obtained was transferred to a fresh tube. Then the active LHRH-PE40 in supernatant was purified by applying to anion exchange chromatography (Amersham Pharmacia) and hydrophobic interaction chromatography (Amersham Pharmacia) according to the manufacturers' instructions. Purity of the fusion protein was analyzed by sodium dodecyl sulfate polyacrylamide gel electrophoresis (SDS-PAGE), and protein concentration was determined by Bradford assay. The molecular weight of LHRH-PE40 by mass chromatographic analysis is about 41 kD (Figure S1, Supporting Information).

PEA is made up of three domains: the binding domain (domain I), the translocation domain (domain II), and the ADP ribosylating elongation factor-2 domain (domain III). PE40, the truncated PEA, retains translocation and ADP ribosylation activity and is usually the toxic part of anticancer drugs.[21,22] The target drug LHRH-PE40 was actually obtained by replacing domain I with LHRH. The active principle of LHRH-PE40 is that its ADP ribosylation fraction (domain III) enters cells through the translocation domain to kill cancer cells after its guide fraction LHRH binds to LHRH-R on the targeted cell membrane surface.

Human LHRH was obtained from Prospec-Tany (Israel), and Hela cells (human carcinoma cervical cells) were purchased from the Cell Bank of Chinese Academy of Science (Shanghai, China).

2.2. Cell Culture. Hela cells were cultivated in T25 culture flasks using Dulbecco's modified Eagle's medium (DMEM; Gibco, USA), supplemented with 10% fetal bovine serum (Hyclone, Lanzhou, China), 100 U mL^{-1} penicillin, 200 μg mL^{-1} streptomycin, and 2 μM L-glutamine in a humidified 5% CO_2 atmosphere at 37 °C. After reaching confluence, cells for force measurement were seeded directly onto 35 mm Petri dishes at a proper cell density for 24 h. Before experiments, the subconfluent cells (about 70−90%) were rinsed 10 times with phosphate buffer saline (PBS; 137 mM NaCl, 2 mM KCl, 8 mM Na_2HPO_4, 1.5 mM KH_2PO_4, and pH 7.4).

2.3. Cell Growth Inhibition Assay. The viabilities of Hela cells after LHRH-PE40 treatment were determined by 3-[4, 5-dimethylthiazol-2-yl]-diphenyltetrazolium bromide (MTT, Sigma) assay. Operatively, cells were seeded in a 96-well plate. After 12 h of culture, cells were treated with LHRH-PE40 at various concentrations for 48 h. All samples had five parallel wells. Then, the culture medium was replaced by 90 μL serum-free appropriate medium and 10 μL MTT solution (5 mg mL^{-1}) and then incubated at 37 °C for 4 h. The reaction solution was carefully aspirated; and 150 μL DMSO was added to dissolve the formazan crystals. The optical density value (Absorbance, Abs) was read by the Multi-Detection Microplate Reader (Power Wave XS2, Bio-Tek Instrument Inc., USA). The inhibition rate of LHRH-PE40 relative to the untreated control cells was calculated as follows:

$$\text{Inhibition rate} = \frac{\text{Abs}_{\text{control cells}} - \text{Abs}_{\text{treated cells}}}{\text{Abs}_{\text{control cells}}} \times 100\% \quad (1)$$

The IC_{50} value was defined as the concentration of LHRH-PE40 needed for a 50% reduction in absorbance based on cell growth curve.

2.4. Fluorescence Imaging. The procedure of fluorescence labeling was according to the product instruction. In brief, Cy5 was conjugated to LHRH-PE40 by incubating LHRH-PE40 (1 mg mL^{-1}) with Cy5-NHS ester (10 mg mL^{-1}, OPE, China) at room temperature with continuously gentle stirring for 2 h. The prepared LHRH-PE40-Cy5 was purified via microcon centrifugal filter devices (Millipore, USA), and added to Hela cells in PBS buffer for 1 h at 37 °C. Subsequently, the cells were rinsed with PBS buffer five times. Fluorescence imaging was performed in PBS buffer on a confocal fluorescence microscopy (CLSM TCS-SP2, Leica, Germany).

2.5. AFM Tip Preparation and Force Measurement. For SMFS, AFM tips (MSCT, Veeco, USA) were functionalized with LHRH or LHRH-PE40 as previously described.[23] After cleaning with ethanol and chloroform, AFM tips were amino-functionalized by incubation with 50 μL of 3-aminopropyltriethoxysilane (APTES) and 15 μL of triethylamine using a vapor deposition method. The 8 nm long heterobifunctional polyethylene glycol cross-linker (NHS-PEG_{18}-aldehyde) was attached to AFM tips by immersing the tips for 2 h with 6.6 mg mL^{-1} of linker in chloroform containing 0.5% (v/v) of triethylamine. The coupling of LHRH or LHRH-PE40 was accomplished by immersing AFM tips in 100 μg mL^{-1} protein (LHRH or LHRH-PE40) in PBS buffer containing 20 mM $NaCNBH_3$. Two hours later, ethanolamine was added to a final concentration of 25 mM to passivate unreacted aldehyde

groups. The tips were washed five times with PBS and stored in PBS at 4 °C.

The force measurements were carried out on PicoSPM 5500 (Agilent Technologies, USA). All SMFS experiments were performed in PBS buffer at 37 °C with contact mode. Hundreds of force−distance curves were collected for one set of measurement. Each set of measurement was performed with a same tip on 6 to 10 different cells, at randomly selected four to six locations on each cell. Loading rates r, were calculated by $r = df/dt = vk_{eff}$, with v being the pulling velocity and k_{eff} being the effective spring constant. The spring constants of the cantilevers were determined by the thermal-noise mode. Analysis of force−distance curves was performed with Matlab 7.1 as previously described.

3. RESULTS AND DISCUSSION

Before performing force spectroscopy, the cell growth inhibition assay was applied to understand the response of Hela cells to LHRH-PE40. The ability of cells to reduce MTT provides an indication of mitochondrial integrity and activity which, in turn, may be interpreted as a measure of cell number/proliferation/viability/toxicity.[24] As shown by the large area in Figure 1A, Hela cells treated with LHRH-PE40 present shrinkage, cytoplasmic dark granularity, and death, comparing with those treated without LHRH-PE40. Additionally, these morphology changes are time-dependent and dose-dependent. Figure 1B depicts the cytotoxicity of LHRH-PE40 qualitatively. The cells exposed to LHRH-PE40 at the concentration of 9.38 μg mL^{-1} for 24 h, can still survive in a low density. However, almost all the cells shrink and die, when exposed to LHRH-PE40 at a concentration of 1.2 mg mL^{-1} for 48h, and the inhibition rate is 95.06%. The IC_{50} value of LHRH-PE40, which causes 50% inhibition of cell growth, is 1.28 μM from the inhibition rate curve. The cytotoxic effect of PE40 without LHRH was also examined under the same experiment conditions (Figure S2). The result shows that PE40 has no cytotoxic effect on Hela cells as a truncated protein with no binding domain. These data suggest LHRH-PE40 has quite specific cytotoxic effects on Hela cells in a very low dose through the LHRH-R pathway.

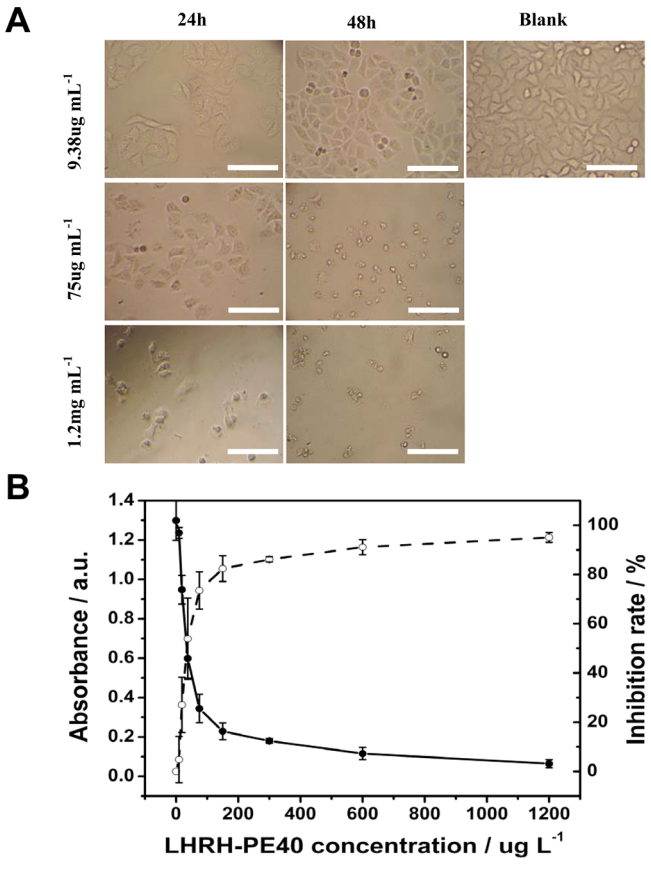

Figure 1. Cytotoxiciy of LHRH-PE40 on Hela cells. (A) Light microscope images of Hela cells exposed to LHRH-PE40 with different concentrations and different times. The scale bar is 100 μm. (B) Growth inhibition curve of LHRH-PE40 to healthy Hela cells. The solid curve (—) presents absorbance of Hela cells at 550 nm after being treated with LHRH-PE40 for 48 h. The dash curve (...) is the inhibition curve derived from the absorbance value.

Fluorescence images were obtained after Hela cells were incubated with Cy5-labed LHRH-PE40 in PBS buffer for 1 h (Figure 2). Very bright red fluorescence is observed, which arises from the Cy5-labed LHRH-PE40 that specifically bound to LHRH-Rs on the cell surface. The fluorescence image (Figure 2A) was merged with the brightfield image that was recorded in the same part with different light pathway (Figure 2B). The fluorescence spots on Hela cells in the merged image distinctly indicate the locations of LHRH-Rs on cell surface at micrometer scale. The results confirm that LHRH-Rs are abundantly expressed by Hela cells and distributed on outer cell membrane. The ability of LHRH moiety of LHRH-PE40 to recognize LHRH-Rs on Hela cell surface is also demonstrated to some extent.

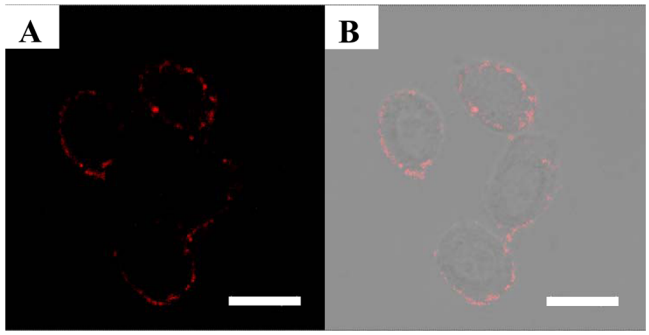

Figure 2. Confocal fluorescence imaging. (A) Confocal fluorescence images of Hela cells incubated with Cy5-labeled LHRH-PE40 for 1 h at 37 °C. (B) The merged image distinctly displays the positions of LHRH-Rs on Hela cells. The scale bar is 20 μm.

SMFS was carried out to probe the interaction between LHRH-PE40 and LHRH-R on living cell surface at the single-molecule level. For this purpose, the LHRH-PE40 molecule was covalently coupled to an amino-functionalized AFM tip via a heterobifunctional polyethylene glycol cross-linker (NHS-PEG_{18}-aldehyde) (Figure 3). The surface density of the ligands on the AFM tip was adjusted such that single molecular detection became highly probable.[23] A typical force−distance curve with a single molecular recognition event on the living cell surface is presented in Figure 4A. Before the tip conjugated with LHRH-PE40 touched the cell surface, no force was transmitted to the tip, which corresponded to a horizontal zero-force line in the right part of the force curve (black line). After bringing the AFM tip to contact the cell surface, the tip indented the cell surface and the force transmitted to the tip increased in a quasi-linear manner. A LHRH-PE40/LHRH-R

dx.doi.org/10.1021/jp306882r | J. Phys. Chem. B 2012, 116, 13331−13337

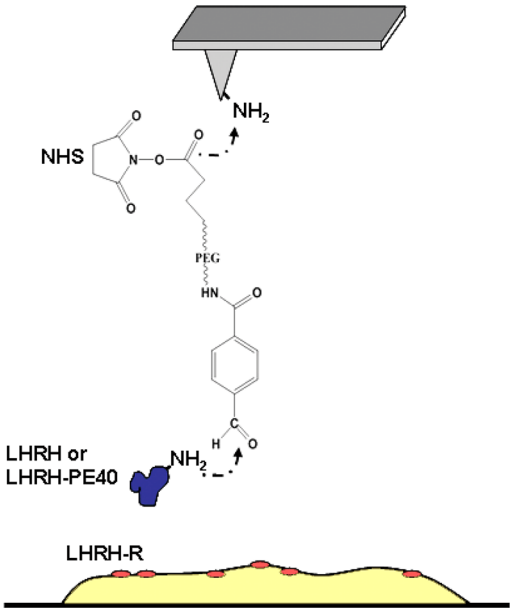

Figure 3. Schematic representation of the experimental procedure. The cross-linker NHS-PEG_{18}-aldehyde is covalently bound to the APTES-coated tip through the NHS-ester end. The protein studied is conjugated to the aldehyde end.

complex formed because the LHRH-PE40 engaged a LHRH-R molecule on the Hela cell surface during the contact period. Subsequently, retracting the tip from cell surface, the indented cell surface relaxed, and a pulling force was gradually loaded in a nonlinear way on the bond of LHRH-PE40/LHRH-R because of the increasing distance between the tip and sample surface (red line). The complex finally broke at a critical point, and the tip jumped back to the rest position. The nonlinear increase of the loading force is accounted for by the elastic extension of the distensible PEG cross-linker through which the LHRH-PE40 was connected to the AFM tip and, more prominent, by the stretching of the highly elastic cellular membrane.[11] The unbinding force at the critical point amounts to ~100 pN. The force retrace shown contained the unique signature of a single-molecule dissociation: the typical unbinding force (~100 pN at the loading rate of 1.18 nN s^{-1}), the typical unbinding length (200 nm—2000 nm), and the characteristic nonlinear force–distance relation of the PEG linker.[25] The addition of 200 μL LHRH-PE40 (1 mg mL^{-1}) into the fluid cell for 60 min led to the disappearance of the specific recognition events in the force–distance curves (Figure 4B), which is attributed to the occupation of the binding sites in LHRH-Rs by free ligands. These prove that the interaction forces recorded between LHRH-PE40 on the tip and LHRH-R on the Hela cell is specific.

Because of the stochastic nature of the unbinding force, the analyses of many force–distance curves are required. Hundreds of curves were collected for each data set under the identical condition with the same tip. A Gaussian of unitary area with the width representing its measuring uncertainty was constructed for each unbinding force. All Gaussians from one experimental setting were accordingly positioned on a force axis. The sum resulted in an experimental probability density function (pdf). Also, it can be viewed as the equivalent of continuous histogram. This approach offers the advantage that data accuracy will be taken into account and binding artifacts can be excluded.[18] Figure 4C summarized the unbinding force distribution that was obtained by constructing the pdf from one data set of the measured unbinding force of LHRH-PE40/LHRH-R. The overall binding probability (probability of finding a rupture event in force–distance curves) for LHRH-PE40 and the LHRH-Rs expressed on Hela cells was about 11.9% (119 unbinding events in 999 curves). On the basis of Poisson statistics, when the binding probability is <30%, >83% of the observed binding events should originate from a single pair of ligand–receptor interactions.[26] The lack of multiple

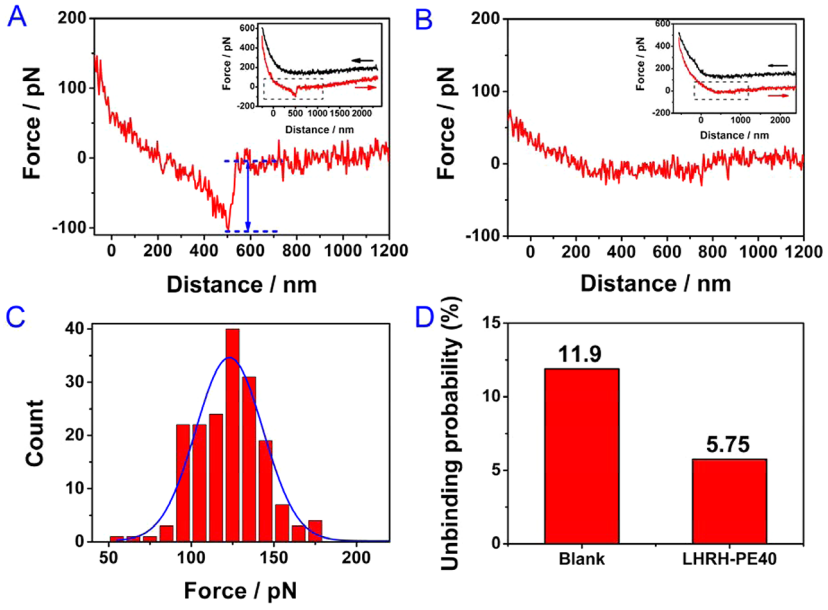

Figure 4. The force measurement on living Hela cells. (A) A typical force–distance cycle with a single molecular recognition event on living cell surface. The addition of free LHRH-PE40 led to the disappearance of the specific recognition event in the force–distance curves (B). (C) The unbinding force distribution of LHRH-PE40/LHRH-R at the retraction speed of (1.18 ± 0.083) nN s^{-1}. (D) The histogram of unbinding probability of LHRH-PE40/LHRH-R before and after free LHRH-PE40 was added.

dx.doi.org/10.1021/jp306882r | J. Phys. Chem. B 2012, 116, 13331–13337

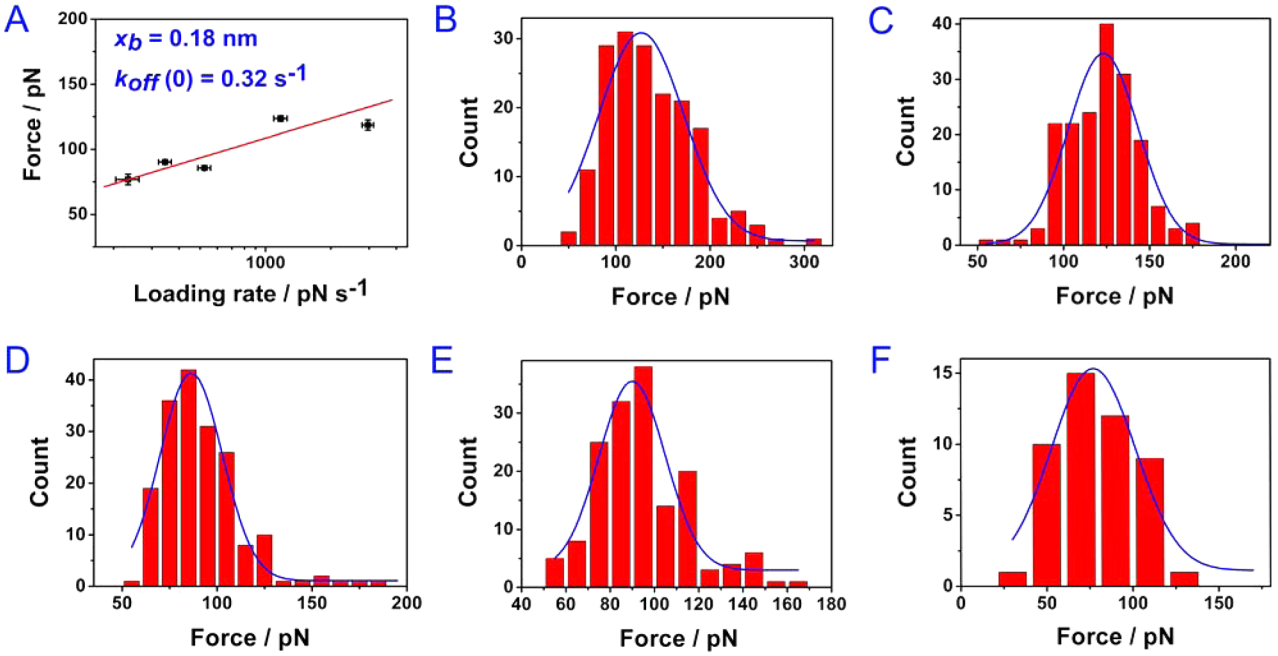

Figure 5. Velocity dependence of the unbinding force of LHRH-PE40/LHRH-R on living Hela cell surfaces. (A) The dependence of the most probable unbinding force (f_u) on the retrace velocity (r). (B−F) The f_u distribution at different loading rates: (2.96 ± 0.18) nN s^{-1}, (1.18 ± 0.083) nN s^{-1}, (0.52 ± 0.035) nN s^{-1}, (0.34 ± 0.023) nN s^{-1}, and (0.23 ± 0.028) nN s^{-1}, respectively.

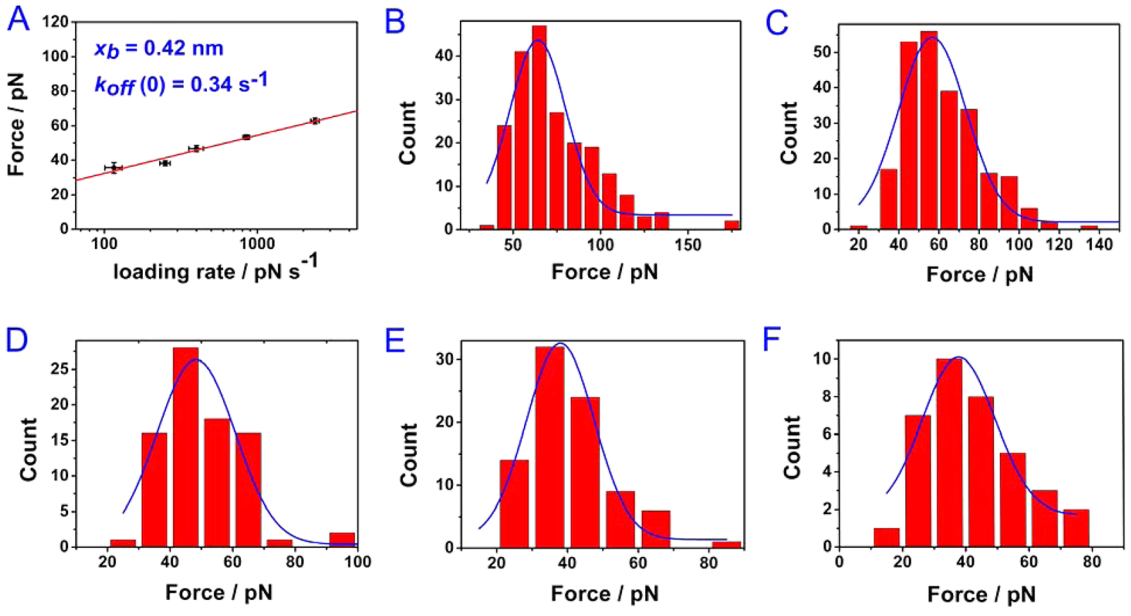

Figure 6. Velocity dependence of the unbinding force of LHRH/LHRH-R on living Hela cells surface. (A) The dependence of the most probable unbinding force (f_u) on the retrace velocity (r). (B−F) The f_u distribution at different loading rates: (2.38 ± 0.15) nN s^{-1}, (0.85 ± 0.042) nN s^{-1}, (0.40 ± 0.044) nN s^{-1}, (0.25 ± 0.019) nN s^{-1}, and (0.12 ± 0.014) nN s^{-1}, respectively.

force peaks in the force distribution also confirms that the measured forces between LHRH-PE40 and LHRH-R were single-molecule interactions. The maximum of the distribution, reflecting the most probable unbinding force of LHRH-PE40/LHRH-R, was (123.58 ± 2.09) pN at a loading rate of (1.18 ± 0.083) nN s^{-1}. After free LHRH-PE40 was added to the fluid cell for 60 min, the binding probability remarkably decreased to about 5.75% (Figure 4D). These results indicate that LHRH-Rs on the Hela cell surface can be specifically detected at the single-molecule level by LHRH-PE40 coupled to AFM tips, and LHRH-Rs are located on the outermost Hela cell surface.

The rupture of weak bonds under a force can be described by treating the unbinding reaction as a probabilistic process induced by a thermal kick over the activation barrier. At very slow force loading rate, the system has simply more attempts to make the transition than at faster force loading rates, and, thus the bond rupture will occur at lower forces than at higher force loading rates.[27] This behavior can be described with the so-called Bell-Evans model,[28] which indicates a linear relationship between the unbinding force and the logarithm of the loading rate r:

dx.doi.org/10.1021/jp306882r | J. Phys. Chem. B 2012, 116, 13331−13337

$$F_u(r) = \frac{k_B T}{x_\beta} \ln\left(\frac{r x_\beta}{k_{off}(0) k_B T}\right) = \frac{k_B T}{x_\beta} \ln r + \frac{k_B T}{x_\beta} \ln\left(\frac{x_\beta}{k_{off}(0) k_B T}\right) \quad (2)$$

Here, χ_β is the distance of the energy barrier to the minimum energy along the separation path, $k_{off}(0)$ is the dissociation rate constant at zero force, $k_B T$ is the thermal energy, and r and f_u are the loading rate and the most probable unbinding force, respectively. The loading rate r is calculated from the retraction velocity v times the effective spring constant k_{eff}. k_{eff} is the slope of the force−distance curve at unbinding, which is comprised of the linear spring constant of the AFM cantilever and the nonlinear spring constant of the PEG cross-linker and the cell surface. As Figure 5 shows, the unbinding forces of LHRH-PE40/LHRH-R vary in the range of 50−150 pN and linearly increase with the logarithm of the loading rate, which is consistent with the dynamic response of other receptor−ligand systems.[14,28] The distance of the energy barrier to the minimum energy value χ_β assessed from the slope is 0.18 nm, while extrapolation of the curve to zero force yields the kinetic off-rate constant of the dissociation at zero force value $k_{off}(0)$ is 0.32 s^{-1}.

In order to comprehend the effect of the toxic fraction PE40 of LHRH-PE40 on the specific binding of LHRH moiety to LHRH-R on the targeted cell surface, the same dynamic force measurement was performed using as-prepared tips with LHRH so as to compare the dynamic force spectra of LHRH-PE40/LHRH-R and LHRH/LHRH-R. As illustrated in Figure 6, the most probable unbinding forces of LHRH/LHRH-R on living Hela cells surface linearly increased with the logarithm of the loading rate, which is the same as that of LHRH-PE40/LHRH-R. However, the most probable unbinding forces for LHRH/LHRH-R are smaller than those of LHRH-PE40/LHRH-R at the almost same loading rate range. Meanwhile, χ_β and $k_{off}(0)$ for the LHRH/LHRH-R complex are 0.42 nm and 0.34 s^{-1}.[29] The similar $k_{off}(0)$ between LHRH-PE40/LHRH-R and LHRH/LHRH-R discloses that the LHRH moiety fused to PE40 protein reserves the ability similar to LHRH to recognize LHRH-R, whereas the higher most probable unbinding force f_u and shorter distance χ_β from the bond state to the energy barrier reveal that LHRH chain becomes more stable after being linked to PE40. f_u is most strongly influenced by the local structure near the mechanical "breakpoint",[30] which is the bond between the LHRH part and LHRH-R. LHRH, a decapeptide sequence, becomes stiffer after being linked to the PE40 part, which results in a shorter distance to the transition state. It was found that[30−32] the more brittle domains (with shorter distances to their transition states) maintain their structure to higher applied forces and only under extreme force conditions would they unfold, while the more compliant domains (having longer distances to their transition states) stretch in response to low applied forces.

4. CONCLUSION

In conclusion, the capability of LHRH-PE40 to recognize LHRH-Rs on a living cell membrane was studied with the help of AFM-based SMFS. The different unbinding forces and recogniton kinetics of LHRH-PE40/LHRH-R with those of LHRH/LHRH-R reveal that the LHRH moiety in recombinant protein LHRH-PE40 reserves the capacity to recognize LHRH-R specifically and becomes more stable. These results imply that recombinant protein LHRH-PE40 can be a promising drug targeting elevated LHRH-R expressed in malignant tumor tissue. The direct examination of the bond holding LHRH-PE40 and LHRH-R at the single biomolecule level in this work constitutes a quantitative report on the use of SMFS for the biodiscovery of new target drugs.

■ ASSOCIATED CONTENT

Supporting Information

The molecular weight of LHRH-PE40, the effect of PE40 to Hela cells, and the overlapped dynamic force spectra of LHRH-PE40/LHRH-R and LHRH/LHRH-R on living Hela cells surface. This material is available free of charge via the Internet at http://pubs.acs.org.

■ AUTHOR INFORMATION

Corresponding Author

*Tel./fax: +86-0431-85262734 (J.T.); 86-0431-85262430 (B.Z.). E-mail: jltang@ciac.jl.cn (J.T.); blzhang@ciac.jl.cn (B.Z.).

Author Contributions

#These authors contributed equally to this paper.

Notes

The authors declare no competing financial interest.

■ ACKNOWLEDGMENTS

This work was supported by the National Basic Research Program of China (No. 2011CB935800), the National Science Foundation of China (Nos. 20735001, 20975096 and 21075121), and the SCIENTIFIC AND TECHNICAL COOPERATION (STC) Austria-Republic of China 2010-2012 (NO. CN 03/2010). We thank Dr. Christian Rankl for the help in analyzing the data.

■ REFERENCES

(1) Dharap, S. S.; Wang, Y.; Chandna, P.; Khandare, J. J.; Qiu, B.; Gunaseelan, S.; Sinko, P. J.; Stein, S.; Farmanfarmaian, A.; Minko, T. *Proc. Natl. Acad. Sci. U.S.A.* **2005**, *102*, 12962−12967.

(2) Sarnovsky, R.; Tendler, T.; Makowski, M.; Kiley, M.; Antignani, A.; Traini, R.; Zhang, J. L.; Hassan, R.; FitzGerald, D. J. *Cancer Immunol. Immun.* **2010**, *59*, 737−746.

(3) Kreitman, R. J.; Stetler-Stevenson, M.; Margulies, I.; Noel, P.; FitzGerald, D. J. P.; Wilson, W. H.; Pastan, I. *J. Clin. Oncol.* **2009**, *27*, 2983−2990.

(4) Kreitman, R. J. *Biodrugs* **2009**, *23*, 1−13.

(5) Onda, M.; Beers, R.; Xiang, L.; Nagata, S.; Wang, Q. C.; Pastan, I. *Proc. Natl. Acad. Sci. U.S.A.* **2008**, *105*, 11311−11316.

(6) Deng, X.; Klussmann, S.; Wu, G. M.; Akkerman, D.; Zhu, Y. Q.; Liu, Y.; Chen, H.; Zhu, P.; Yu, B. Z.; Zhang, G. L. *J. Drug Target.* **2008**, *16*, 379−388.

(7) Kreitman, R. J.; Squires, D. R.; Stetler-Stevenson, M.; Noel, P.; Fitzgerald, D. J. P.; Wilson, W. H.; Pastan, I. *J. Clin. Oncol.* **2005**, *23*, 6719−6729.

(8) Dharap, S. S.; Minko, T. *Pharm. Res.* **2003**, *20*, 889−896.

(9) Gong, S. L.; Zhao, G.; Zhao, H. G.; Lu, W. T.; Liu, G. W.; Zhu, P. *World J. Gastroenterol.* **2004**, *10*, 2870−2873.

(10) Muller, D. J.; Krieg, M.; Alsteens, D.; Dufrene, Y. F. *Curr. Opin. Biotechnol.* **2009**, *20*, 4−13.

(11) Wildling, L.; Rankl, C.; Haselgrübler, T.; Gruber, H. J.; Holy, M.; Newman, A. H.; Zou, M.-F.; Zhu, R.; Freissmuth, M.; Sitte, H. H.; et al. *J. Biol. Chem.* **2012**, *287*, 105−113.

(12) Shan, Y.; Huang, J.; Tan, J.; Gao, G.; Liu, S.; Wang, H.; Chen, Y. *Nanoscale* **2012**, *4*, 1283−1286.

(13) Shan, Y.; Ma, S.; Nie, L.; Shang, X.; Hao, X.; Tang, Z.; Wang, H. *Chem. Commun.* **2011**, *47*, 8091−8093.
(14) Li, Y. J.; Wang, J. N.; Xing, C. Y.; Wang, Z. X.; Wang, H. D.; Zhang, B. L.; Tang, J. L. *ChemPhysChem* **2011**, *12*, 909−912.
(15) Zhu, R.; Howorka, S.; Proll, J.; Kienberger, F.; Preiner, J.; Hesse, J.; Ebner, A.; Pastushenko, V. P.; Gruber, H. J.; Hinterdorfer, P. *Nat. Nanotechnol.* **2010**, *5*, 788−791.
(16) Yu, J.; Wang, Q.; Shi, X.; Ma, X.; Yang, H.; Chen, Y.-G.; Fang, X. *J. Phys. Chem. B* **2007**, *111*, 13619−13625.
(17) Gilbert, Y.; Deghorain, M.; Wang, L.; Xu, B.; Pollheimer, P. D.; Gruber, H. J.; Errington, J.; Hallet, B.; Haulot, X.; Verbelen, C.; et al. *Nano Lett.* **2007**, *7*, 796−801.
(18) Hinterdorfer, P.; Baumgartner, W.; Gruber, H. J.; Schilcher, K.; Schindler, H. *Proc. Natl. Acad. Sci. U.S.A.* **1996**, *93*, 3477−3481.
(19) Florin, E. L.; Moy, V. T.; Gaub, H. E. *Science* **1994**, *264*, 415−417.
(20) Binnig, G.; Quate, C. F.; Gerber, C. *Phys. Rev. Lett.* **1986**, *56*, 930−933.
(21) Hwang, J.; Fitzgerald, D. J.; Adhya, S.; Pastan, I. *Cell* **1987**, *48*, 129−136.
(22) Pastan, I.; Chaudhary, V.; FitzGerald, D. J. *Annu. Rev. Biochem.* **1992**, *61*, 331−354.
(23) Ebner, A.; Wildling, L.; Kamruzzahan, A. S. M.; Rankl, C.; Wruss, J.; Hahn, C. D.; Hölzl, M.; Zhu, R.; Kienberger, F.; Blaas, D.; et al. *Bioconjugate Chem.* **2007**, *18*, 1176−1184.
(24) Maioli, E.; Torricelli, C.; Fortino, V.; Carlucci, F.; Tommassini, V.; Pacini, A. *Biol. Proced. Online.* **2009**, *11*, 227−240.
(25) Riener, C. K.; Stroh, C. M.; Ebner, A.; Klampfl, C.; Gall, A. A.; Romanin, C.; Lyubchenko, Y. L.; Hinterdorfer, P.; Gruber, H. J. *Anal. Chim. Acta* **2003**, *479*, 59−75.
(26) Tees, D. F. J.; Waugh, R. E.; Hammer, D. A. *Biophys. J.* **2001**, *80*, 668−682.
(27) Evans, E.; Ritchie, K. *Biophys. J.* **1997**, *72*, 1541−1555.
(28) Shi, X. L.; Xu, L.; Yu, J. P.; Fang, X. H. *Exp. Cell Res.* **2009**, *315*, 2847−2855.
(29) Fang, X.; Yu, J.; Jiang, Y.; Ma, X.; Lin, Y. *Chem. Asian J.* **2007**, *2*, 284−289.
(30) Bustamante, C.; Chemla, Y. R.; Forde, N. R.; Izhaky, D. *Annu. Rev. Biochem.* **2004**, *73*, 705−748.
(31) Li, H. B.; Linke, W. A.; Oberhauser, A. F.; Carrion-Vazquez, M.; Kerkviliet, J. G.; Lu, H.; Marszalek, P. E.; Fernandez, J. M. *Nature* **2002**, *418*, 998−1002.
(32) Oberhauser, A. F.; Badilla-Fernandez, C.; Carrion-Vazquez, M.; Fernandez, J. M. *J. Mol. Biol.* **2002**, *319*, 433−447.